Chemical Engineering Journal 242 (2014) 170–179

Contents lists available at ScienceDirect

Chemical Engineering Journal

journal homepage: www.elsevier.com/locate/cej

Ion-exchange resin catalyzed transesterification of ethyl acetate with methanol: Gel versus macroporous resins

Evelien Van de Steene [a,b], Jeriffa De Clercq [a], Joris W. Thybaut [b,*]

[a] Department of Industrial Technology & Construction, Ghent University, Valentin Vaerwyckweg 1, B-9000 Ghent, Belgium
[b] Laboratory for Chemical Technology, Ghent University, Technologiepark 914, B-9052 Zwijnaarde, Belgium

HIGHLIGHTS

- Resin swelling determines active site accessibility and, hence, catalytic activity.
- Gel resins outperform macroporous ones in ethyl acetate transesterification with methanol.
- The kinetic model implicitly accounts for swelling by assuming full active site coverage.
- Protonated ethyl acetate reaction with bulk methanol is rate determining.
- The selected Eley–Rideal mechanism is independent of the resin used.

GRAPHICAL ABSTRACT

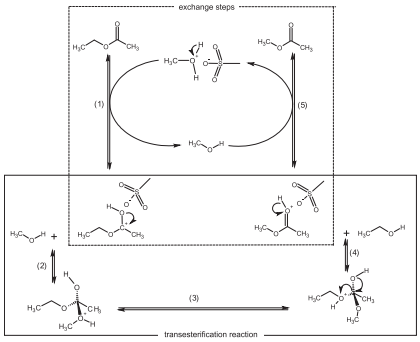

ARTICLE INFO

Article history:
Received 26 September 2013
Received in revised form 7 December 2013
Accepted 10 December 2013
Available online 25 December 2013

Keywords:
Heterogeneous catalysis
Transesterification
Ion-exchange resin
Kinetics
Cross-linking density
Swelling

ABSTRACT

The liquid-phase transesterification kinetics of ethyl acetate with methanol to ethanol and methyl acetate catalyzed by gel (Lewatit K1221) and macroporous (Lewatit K2640, Lewatit K2629 and Amberlyst 15) ion-exchange resins have been investigated. The effects of the resins' swelling, the initial reactant molar ratio (1:1–10:1) and the temperature (303.15–333.15 K) on the reaction kinetics were assessed. Macroporous Lewatit K2629, Lewatit K2640 and Amberlyst 15 exhibit a clearly inferior catalytic activity compared to the gel type Lewatit K1221, despite the similar number of sulfonic acid active sites. This trend in catalytic activity can be explained by the differences in acid site accessibility, which are related to the resins' swelling behavior and, hence, the extent of divinylbenzene cross-linking in the polymeric structure. A fundamental kinetic model, accounting for the chemical elementary steps as well as for the physical swelling due to solvent sorption, was constructed. According to this model (1) all active sites are initially occupied by protonated methanol, (2) the esters are activated by a proton exchange with protonated methanol and (3) the reaction occurs through an Eley–Rideal mechanism with the surface reaction of protonated ethyl acetate with methanol from the bulk as the rate-determining step. The kinetic model adequately described the experimental data as a function of temperature, initial molar ratio and catalyst resin type. A value of 49 kJ mol^{-1} was obtained for the activation energy, irrespective of the resin used. Differences in catalytic activity caused by the accessibility of the active sites are reflected by the values obtained for the reaction rate coefficient, which is 3–4-fold higher for a gel type resin compared to the macroporous ones.

1. Introduction

Esterification and transesterification reactions are widely used for the synthesis of fine chemicals, pharmaceuticals, plastics

* Corresponding author. Tel.: +32 9 331 17 52; fax: +32 9 331 17 59.
E-mail address: Joris.Thybaut@Ugent.be (J.W. Thybaut).

1385-8947/$ - see front matter © 2013 Elsevier B.V. All rights reserved.
http://dx.doi.org/10.1016/j.cej.2013.12.025

Nomenclature

a_i	activity of component i
A	pre-exponential factor (mol kg_{cat}^{-1} s^{-1})
b	parameter estimate
C_i	observed concentration of component i (mol m^{-3})
$\widehat{C}_i$	predicted concentration of component i (mol m^{-3})
E_A	activation energy (kJ mol^{-1})
k_{SR}	surface reaction rate coefficient (mol g_{cat}^{-1} s^{-1})
K_{eq}	equilibrium coefficient of the overall reaction
K_i	adsorption/exchange equilibrium coefficient of component i (m^3 mol^{-1}) (–)
m_i	mass of component i (kg)
n_i	number of moles of component i (mol)
N	total number of experimental points or components
p	number of parameters
r	reaction rate (mol kg_{cat}^{-1} s^{-1})
R_i	net production rate of component i (mol kg_{cat}^{-1} s^{-1})
RSSQ	residual sum of squares
S	swelling ratio
t	time (s)
T	temperature (K)
W	weight of catalyst (kg_{cat})
X_i	conversion of component i

Greek symbols

β	parameter
γ_i	activity coefficient of component i
θ_i	fractional coverage of catalyst surface by component i
ν_i	stoichiometric coefficient for component i

Subscripts and superscripts

0	initial conditions
cat	catalyst
eq	at equilibrium
i	component i
T_{ref}	at reference temperature

monomers, and many other products [1,2]. The significant expansion of the biodiesel production capacity in the last decade has reinforced the interest in both reactions and the optimization of their industrial implementation.

Transesterification reactions can be performed using base catalysts, such as metal hydroxides, metal alkoxides, alkaline-earth oxides or hydrotalcites or using acid catalysts, such as sulphuric, sulfonic, phosphoric, hydrochloric acids and acid ion-exchange resins [3]. Amongst this wide variety of catalysts, acid ion-exchange resins are gaining popularity as transesterification catalyst [4], as they are ecofriendly, noncorrosive, heterogeneous and have a good stability and reusability. Transesterification has been investigated both in a qualitative as a quantitative manner [4–15]. Pseudo-homogeneous (PH) as well as adsorption-based mechanisms, such as Eley–Rideal (ER) and Langmuir–Hinshelwood (LH) mechanisms have been used for this purpose [6,13,14,16]. The most commonly used one is the simpler pseudo-homogeneous model that gave similar simulation results as the Langmuir–Hinshelwood model [14]. However, pseudo-homogeneous models lack any adsorption or swelling phenomena and, hence, more advanced models are required when assessing the kinetics on a series of heterogeneous catalysts with varying properties, such as the resins considered in the present work.

Swelling due to solvent sorption is of particular importance in the use of ion-exchange resins [17,18]. When a dry resin, which inherently has a very low surface area, is brought into contact with a solvent, it can swell. The solvent is sorbed by the resin until equilibrium is reached with the liquid bulk phase. Because of the flexible structure of the polymeric resin, its volume increases during solvent sorption. When, e.g., water diffuses into the resin, it interacts with its sulfonic acid sites, forms protonated water molecules and primary solvation shells. As a consequence of this solvation additional water molecules are attracted into the gel phase and further extend the solvation shell. This phenomenon is observed at the macro scale as the swelling of the resin, thanks to the elastic properties of the polymeric network [17,19,20].

When contacted with multicomponent mixtures, different components tend to sorb on a resin to a different extent [19,21–24]. Sorption results in significant partitioning of the components between the bulk phase on the one hand and the resin on the other. The partitioning as well as the resins' swelling depend on the physicochemical characteristics of the components and the resin involved. These include not only the liquid phase composition and temperature but also the functional groups and the structure of the polymeric resin, i.e. type of polymer, polystyrene or polyacrylic and degree of cross-linking [24].

A comprehensive theory for describing sorption and swelling behavior of various components on a wide range of resins, related to resin catalyzed kinetics is not available yet [25]. Nevertheless, for the esterification of free fatty acids with methanol, Tesser et al. [17] accounted already for swelling phenomena in their kinetic model, by the use of a physical phase equilibrium relationship between the resin-absorbed and the external liquid phase.

Two types of morphology in cross-linked polymer resins are commercially available and have been investigated: a gel type such as Lewatit K1221 and macroporous type resins such as Lewatit K2640, Lewatit K2629, and Amberlyst 15. Gel type resins are available as a hard glassy transparent resin bead which consists of a homogeneous matrix on a microscopic scale without discontinuities [4]. When dry, it has a very low surface area: typically less than 10 m^2 g^{-1} as measured by BET. Even small molecules diffuse very slowly through this polymeric resin, which does not have permanent pores. As described above, these resins swell when brought into contact with a solvent, with the swelling degree typically being inversely related to the divinylbenzene (DVB) content. Swelling creates space or 'solvent porosity' inside the resin and allows ready access to the polymer network for small molecules [26]. A macroporous type resin, on the other hand, is available as a hard opaque bead which has permanent pores and is relatively rigid. Hence, it typically exhibits a less pronounced swelling behavior compared to a gel type resin. The polymer matrix can be regarded as a conglomerate of permanent macropores and small gel particles. As a result, these materials have much higher surface areas in the dry state, typically ranging from ~50–1000 m^2 g^{-1}, and allow already more easy access to their interior without swelling [26]. The macropore structure does not appreciably vary with the solvent [27]. Nevertheless, when a macroporous resin is contacted with a solvent gel particle swelling occurs to some extent [26]. Studies on the kinetics of the acetic acid and amyl alcohol esterification catalyzed by gel and macroporous resins [9,28] typically observed a higher activity of the gel type resin versus the macroporous one, e.g. Amberlyst 15.

Several authors have reported that esterification reactions, catalyzed by macroporous ion-exchange resins, occur on the functional groups in the small gel particles of the resin [21,24,26,29]. For the esterification of phenol and acetic acid, Ihm et al. [30] found that the conversion increased with the resins' swelling capability. It was, hence, concluded that the reactant molecules can

Table 1
Chemical and physical properties of ion-exchange resins used in ethyl acetate transesterification with methanol at the operating conditions reported in Table 2.

Property	K1221	K2629	K2640	Amberlyst 15
Appearance	Dark brown, translucent	Beige, opaque	Beige, opaque	Deep grey-beige
Type	Gel	Macroporous	Macroporous	Macroporous
Acidic site[a] (eq/kg)	5.3	4.8	5.2	4.8
% DVB	4%	18%	18%	20%
Bead size (mm)	0.4–1.25	0.4–1.2	0.4–1.25	0.3–1.2
Sulfonation degree	Stoichiometric	Stoichiometric	Poly	Stoichiometric

[a] Determined on the dry form of the resin.

move more easily into the swollen gel particle, and that the reaction occurs also on the internal functional groups.

The aim of this work is to elucidate the effect of temperature and alcohol to ester initial molar ratio on the transesterification of methanol with ethyl acetate, on four acid ion-exchange catalysts, i.e. one gel and three macroporous type resins. A novel kinetic model, that also takes the swelling into account and which is applicable to all considered resins, is developed based on an ion-exchange rather than an adsorption mechanism.

2. Procedures

2.1. Chemicals and catalysts

Methanol (Fiers, purity > 99.85%) and ethyl acetate (Fiers, purity $\geqslant$ 99.5%) were used as reagents as received. *n*-Octane (Acros Organics, purity > 99%) was used as internal standard.

The ion-exchange resins Lewatit K1221, Lewatit K2640, Lewatit K2629 (Lanxess) and Amberlyst 15 (Rohm & Haas) are spherical polystyrene-based resin beads that are crosslinked with divinylbenzene and that have sulfonic acid groups as active centers. The resins' properties are reported in Table 1. Prior to transesterification, the resins were freeze dried under vacuum at 233 K for 24 h to completely remove any moisture, as advised by the suppliers.

2.2. Volumetric swelling tests

Several authors [23,24,31–33] have already used volumetric swelling tests to determine, in a fast and simple way, resin swelling. The swelling ratio is determined as the ratio of the volume of the swollen resin, in the presence of a solvent, to the volume of the dry resin. A graduated cylinder of 25 mL was filled with 10 mL of dry resin and subsequently 25 mL of solvent was added. A steady level was obtained in less than 1 minute. The volume of the wet resin was read and the swelling ratio *S*, i.e., ratio of swollen resin volume to dry resin volume, was calculated. No effect of compressibility was observed when using graduated cylinders of different diameter.

2.3. Intrinsic kinetics measurements

The experimental set-up and operating procedures have been described in more detail as part of previous work [5]. All experiments have been performed at atmospheric pressure. Each experiment was performed at least quadruple with an experimental error below 5%. The range of experimental conditions is given in Table 2. The total reaction volume was held constant, at 0.185×10^{-3} m^3. Hence, when varying the initial molar ratio, a change in amount of both reagents was required. An initial data set was acquired by systematically varying the operating conditions and was complemented by experiments where the conditions were selected via design of experiments [5].

Table 2
Range of experimental conditions used in ethyl acetate transesterification with methanol on the ion-exhange resins reported in Table 1.

Temperature (K)	303.15–333.15
Pressure (MPa)	0.1
MeOH:EtOAc molar ratio	1:1–10:1
Catalyst mass (10^{-3} kg)	0.5–5.0
Experiment time (s)	0.0–25,000.0
Batch time[a] (kg s)	0.0–126.0

[a] Defined as product of experiment time multiplied by the mass of catalyst.

In order to ascertain that the obtained data represent intrinsic kinetics, they should be free from deviations due to non-ideal reactor hydrodynamics and interference with transport phenomena. This was verified by Van de Steene et al. [5] based on numerical criteria for all types of potential transport limitations as well as on qualitative tests for the absence of internal and external mass-transfer resistances. Samples of the reaction mixture were withdrawn through the sampling port every 1800 s, and were analyzed by gas chromatography with a Stabilwax capillary column and a flame ionization detector. Only experiments with a mass balance deviation below 5% were used in the kinetic modeling. Prior to any regression, the corresponding experimental results were scaled to obey a 100% mass balance.

2.4. Thermodynamic calculations

The reaction enthalpy was calculated based on thermodynamic data obtained from the tabulated values of the NIST Chemistry Webbook, and was found to vary from −4.20 at 303 K to −0.50 kJ/mol at 333 K, showing a slightly exothermic reaction. The corresponding equilibrium coefficient K_{eq} ranges from 1.59 at 303 K to 1.46 at 333 K, which is similar to values reported in previous transesterification studies [2].

Due to the non-ideal character of the reaction mixture, activity coefficients γ_i for each component i were calculated at temperatures ranging from 303 K to 333 K with the UNIFAC group contribution method [34].

2.5. Modeling and regression analysis

The mass balance for species i in a batch reactor, which is considered to be spatially uniform in composition and temperature, is given by:

$$\frac{1}{W}\frac{dn_i}{dt} = R_i = \nu_i r \tag{1}$$

with R_i the specific net production rate of component i, W the catalyst mass in the reactor, ν_i the stoichiometric coefficient of component i, n_i the number of moles of component i in the reaction mixture, t the time and r the reaction rate.

The net production rate is a function of the rate and equilibrium coefficients and the species' activities. The temperature dependence of the rate coefficient is described by the Arrhenius relationship, which is reparameterized according to Kittrell and Pinto [35] to avoid strong binary correlation between the Arrhenius parameters.

Based on the activation energy and the rate coefficient at the reference temperature as well as the adsorption or exchange

Table 3
Swelling ratio (S) of the resins reported in Table 1 when in contact with the pure reactants and products in ethyl acetate transesterification with methanol. The dielectric constants of these reactants and products are also added for comparison.

Swelling ratio	MeOH	EtOH	EtOAc	MeOAc
K1221	2.45 ± 0.07	2.34 ± 0.04	1.23 ± 0.04	1.24 ± 0.05
K2640	1.55 ± 0.05	1.56 ± 0.01	1.33 ± 0.03	1.32 ± 0.03
K2629	1.49 ± 0.08	1.50 ± 0.02	1.30 ± 0.03	1.32 ± 0.03
Amberlyst 15	1.43 ± 0.06	1.50 ± 0.03	1.35 ± 0.02	1.33 ± 0.07
Dielectric constant	32.7	24.5	6.02	6.70

equilibrium coefficients have been determined from regression by minimizing the following objective function:

$$\sum_{k=1}^{N}\left(C_{EtOAc,k}-\widehat{C}_{EtOAc,k}\right)^2 \xrightarrow{b} \text{minimum} \quad (2)$$

with $C_{EtOAc,k}$ the experimentally observed concentration of ethyl acetate in the k^{th} experiment and $\widehat{C}_{EtOAc,k}$ the corresponding, model calculated value, N the total number of experimental measurements and b the parameter vector [14,36]. The minimization was achieved by a single response Levenberg–Marquardt algorithm as implemented in Athena Visual Studio [37]. The residual sum of squares (RSSQ) equals the final value of the objective function of Eq. (2). The global and individual significance of the regression and the parameters was assessed with respectively the F test and t test. Moreover, the regression results were also evaluated based on the physicochemical meaning of the parameter estimates [5]. Apart from the number of adjustable parameters, model discrimination was performed also based on the statistical and physical significance of the individual parameters as well as of the model as a whole.

3. Experimental results

3.1. Volumetric swelling tests

The volumetric swelling tests, see Table 3, indicate that resins' swelling is more pronounced when it is in contact with an alcohol compared to an ester. For the gel type resin, K1221, the swelling ratio nicely follows the dielectric constant of the considered components. This overall trend is preserved for the macroporous resins, however, due to their more rigid structure, swelling is less pronounced, compared to a gel type resin, especially in solvents with a high dielectric constant.

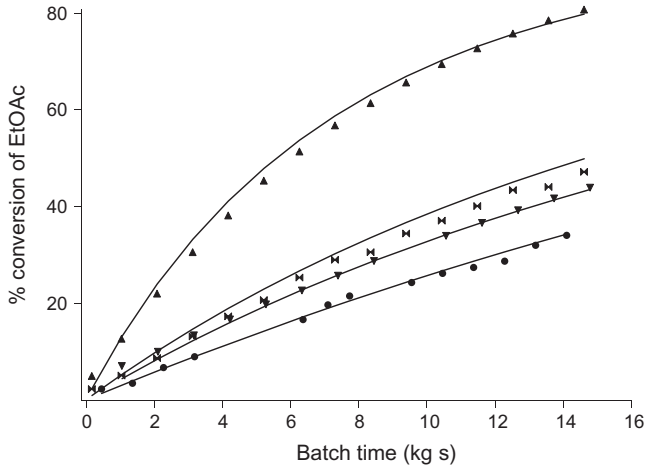

Fig. 1. Simulated (ER_exchange model, Eq. (4), with parameters as reported in Table 5) (lines) and experimental (symbols) conversion of ethyl acetate as a function of the batch time catalyzed by gel and macroporous ion-exchange resins reported in Table 1 (▲ K1221, ▼ K2629, ⋈ K2640, ● Amberlyst 15). (Initial molar ratio of MeOH:EtOAc = 10:1, Temperature = 333 K).

Several factors potentially determine the swelling phenomenon [17], i.e., (1) the nature of the solvent: polar or apolar; (2) the degree of cross-linking of the resin; (3) the nature of the functional groups in the resin and (4) the resins' exchange capacity. For the resins considered in the present work, factors (1) and (2) are invoked to explain the observations. The more polar the solvent, and, hence, the higher the dielectric constant, the higher the swelling ratio, whereas increased cross-linking results in a decrease of the swelling ratio. Various authors reported similar results for the effect of the solvent polarity and the degree of cross-linking [9,14,21,24,33,38–42].

3.2. Catalytic activity

The catalytic activity of the 4 ion-exchange resins for transesterification is shown in Fig. 1. Lewatit K1221 exhibits a noticeably higher activity than the other resins, despite the comparable active site concentration, see Table 1. The catalytic activity of K2629 and K2640 is rather similar while the lowest transesterification rates are observed with Amberlyst 15.

The reaction rate depends on the number of active sites, their acid strength and their accessibility. Because no proportionality is observed between the initial reaction rate, i.e. the slope of the concentration profile at time zero, and the number of active sites, particularly their accessibility, as affected by differences in swelling behavior, and, to a minor extent, their strength are considered to be the determining factors in the observed activity.

From the above mentioned factors the accessibility is indeed significantly affected by the swelling behavior. The latter can easily be related to the divinylbenzene content, c.q., the cross-linking degree. When dry Lewatit K1221 gel beads are placed in a polar reaction medium such as methanol, swelling with ca. 145% of its initial volume occurs and, hence, all the active sites in the body of the bead and on the beads' surface are available for reaction [43]. When, on the other hand, dry macroporous resins, such as Lewatit K2640, K2629 or Amberlyst 15, are placed in a polar reaction medium, swelling with only ca. 55% occurs. The reactants have easy access to the macropores of the bead, c.q., the external active sites of the gel particles [27], but experience severe constraints for entering the small gel particles, and accessing the internal active sites, see Fig. 2. Hence, only the active sites on the surface, in the macropores and in the swollen part of the small gel particles are considered to be available for reaction. The catalytic activity exhibited by the resins is inversely related to their DVB: the gel type resin with 4% DVB has the highest catalytic activity, followed by the macroporous resins with 18% DVB, while the macroporous type with 20% DVB has the lowest catalytic activity. Gusler et al. [20] and Coutinho et al. [33] also found that the exchange capacity is directly proportional to resins' swelling.

Although the DVB content of K2640 and K2629 is identical and amounts to 18%, K2640 is slightly more catalytically active. This can be attributed to the slight differences in acid strength between both resins due to the polysulfonation of Lewatit K2640. Siril et al. [44] observed that the acid strength of sulfonic groups on a polysulfonated resin, which has more than one sulfonic group per styrene unit, is slightly higher than stoichiometrically sulfonated resins such as Amberlyst 15, Lewatit K1221, and Lewatit K2629. A possible explanation lies in the formation of clustered sulfonic acid groups, in which hydrogen bonding between neighboring groups enhances the acid strength [44–46].

The temperature effect was investigated for both gel and macroporous resins in the range from 303 to 333 K. No peculiar adsorption/swelling effects were observed with the temperature and, hence, as expected a higher ethyl acetate conversion was observed at higher temperatures at the same batch time, see Fig. 3.

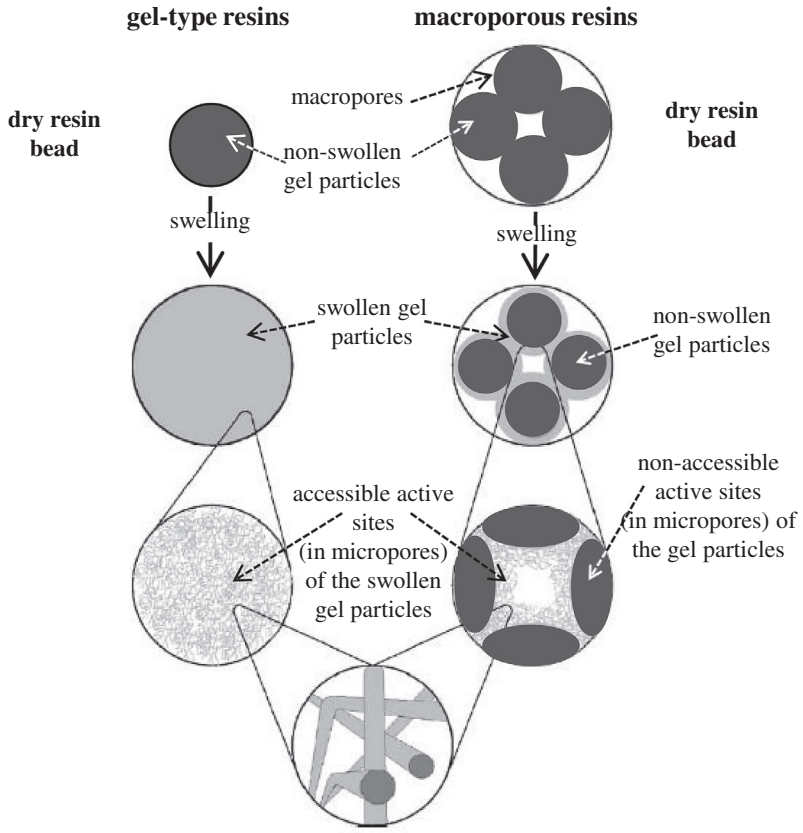

Fig. 2. Schematic representation of the micro- and nanoscale morphology of gel and macroporous resins [43].

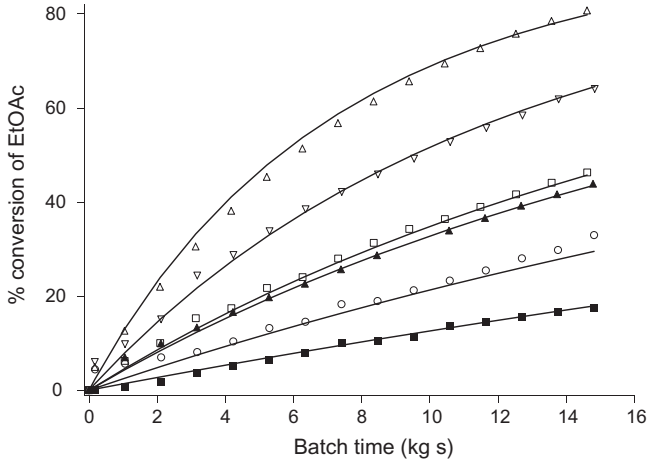

Fig. 3. Simulated (ER_exchange model, Eq. (4), with parameters as reported in Table 5) (lines) and experimental (symbols) conversion of ethyl acetate as function of the batch time catalyzed by gel (K1221) (empty symbols) and macroporous (K2629) (full symbols) ion-exchange resins (Temperature: ○ 303 K; □ 313 K; ▽ 323 K; △ 333 K) (Molar ratio MeOH:EtOAc = 10:1).

The effect of the initial methanol to ethyl acetate ratio (1:1–10:1) was also investigated. An increase in the reactant methanol, expressed by a higher initial molar ratio, result in higher ethyl acetate conversions, see Fig. 4. Because the ethyl acetate/catalyst amount ratio was kept constant in the experiments, this also corresponds to higher specific reaction rates. If the initial molar ratio increases from 1:1 to 5:1, an increase in the initial reaction rate for K1221 and K2640 of respectively a factor 2.0 and 1.5 is obtained. For an increase in the initial molar ratio from 5:1 to 10:1, the initial reaction rate increases for both resins with a factor 1.4.

These differences can be explained by the combination of a different swelling ratio and reactant excess, c.q., methanol. At an initial molar ratio of 1:1 the reaction medium is, due to the small amount of methanol, less polar than at higher molar ratios. A more polar medium increases the resins' swelling and, hence, the accessibility of the active sites [4]. Some additional experimental volumetric swelling tests (not discussed in Section 3.1) performed with the gel type resin K1221, show indeed an increase of the swelling ratio from 1.6 to 2.5 if the initial molar ratio increases from 1:1 to 10:1. For the macroporous resin Lewatit K2640, no significant increase in swelling ratio (S = 1.5) was observed with the initial reactant molar ratio. The swelling ratio is limited to a maximum value of 1.5 even in a more polar solution or in pure methanol, see Table 3. Hence, for Lewatit K2640 the increase in initial reaction rate, with an increase in initial molar ratio, can be entirely attributed to the excess of methanol.

4. Kinetic modeling of gel and macroporous resin catalyzed transesterification

The actual transesterification reaction mechanism comprises first the protonation of the carboxyl group of the ethyl acetate by the acid site. Subsequently, the formed protonated methyl acetate undergoes a deprotonation to regenerate this acid site [5,7,15,32,47–51]. Alonso et al. [7] and Van de Steene et al. [5] found that these protonation and deprotonation steps must be taken into account in the kinetic model for an adequate, physically reasonable representation of the occurring phenomena. In the pseudo-homogeneous model, the interaction (protonation and deprotonation) between component and resin is only implicitly included in the reaction rate coefficient.

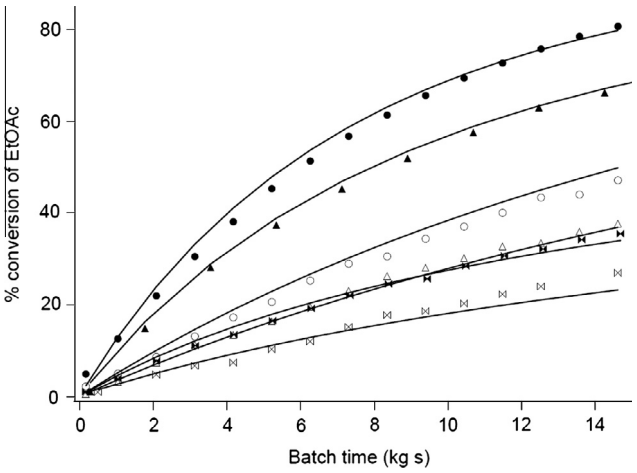

Fig. 4. Simulated (ER_exchange model, Eq. (4), with parameters as reported in Table 5) (lines) and experimental (symbols) conversion of ethyl acetate as a function of the batch time catalyzed by gel (K1221) (closed symbols) and macroporous (K2640) ion-exchange resins (open symbols) (Initial molar ratios MeOH:EtOAc ● 10:1, ▲ 5:1, ⋈ 1:1) (temperature = 333 K).

4.1. Mathematical representation of the resins' swelling behavior in the rate equation

Two alternative ways for representing the adsorption/swelling phenomena are assessed in the present work. First conventional adsorption mechanisms are elaborated, while subsequently a more specific exchange based model is handled in which it is assumed, in accordance with the swelling phenomenon, that all accessible active sites are always occupied.

4.1.1. Adsorption based model

Different authors used the adsorption-based mechanisms such as Eley–Rideal (ER) and the Langmuir–Hinshelwood (LH) to describe the heterogeneously acid ion-exchange catalyzed transesterification [5,6,12–14,52,53].

In previous work, Van de Steene et al. [5] identified an Eley–Rideal based model for transesterification on K1221 with the reaction of adsorbed methanol on the catalyst's active site with ethyl acetate reacting from the bulk as rate-determining step, to form adsorbed ethanol and methyl acetate released to the bulk, as the best performing one amongst a set of 12 competitive equations:

$$r = \frac{k_{SR} K_{MeOH} \left(a_{MeOH} a_{EtOAc} - \frac{1}{K_{eq}} a_{MeOAc} a_{EtOH} \right)}{1 + K_{MeOH} a_{MeOH} + K_{EtOH} a_{EtOH}} \tag{3}$$

with k_{SR} the rate coefficient, a_i the activity of component i, K_{eq} the global equilibrium coefficient and K_i the adsorption equilibrium coefficient of component i. More simple models, such as the pseudo-homogeneous one, were rejected based on their lack of accounting for adsorption and swelling phenomena, despite their good statistical performance based on the F value for the global significance of the regression [5].

The following fundamental interpretation of the transesterification reaction mechanism on Lewatit K1221 was made. First, methanol was physisorbed on the active site, followed by the reaction with protonated ethyl acetate, to form protonated methyl acetate and physisorbed ethanol. Methanol physisorption being more pronounced than physisorption/protonation of ethyl acetate, resulted in an expression for the denominator of the overall rate equation including an adsorption term for methanol but not for ethyl acetate. Without performing dedicated swelling experiments at that time, the strong adsorption of these polar compounds was, hence, also found by Van de Steene et al. [5] and accounted for in their proposed kinetic model (Eq. (3)) and corresponding reaction mechanism as methanol physisorption.

Although such models are commonly used to describe the transesterification reaction kinetics with ion-exchange resins, they do not explicitly account for the swelling behavior of these polymeric resins. As a consequence, an enhanced version of Eq. (3) is

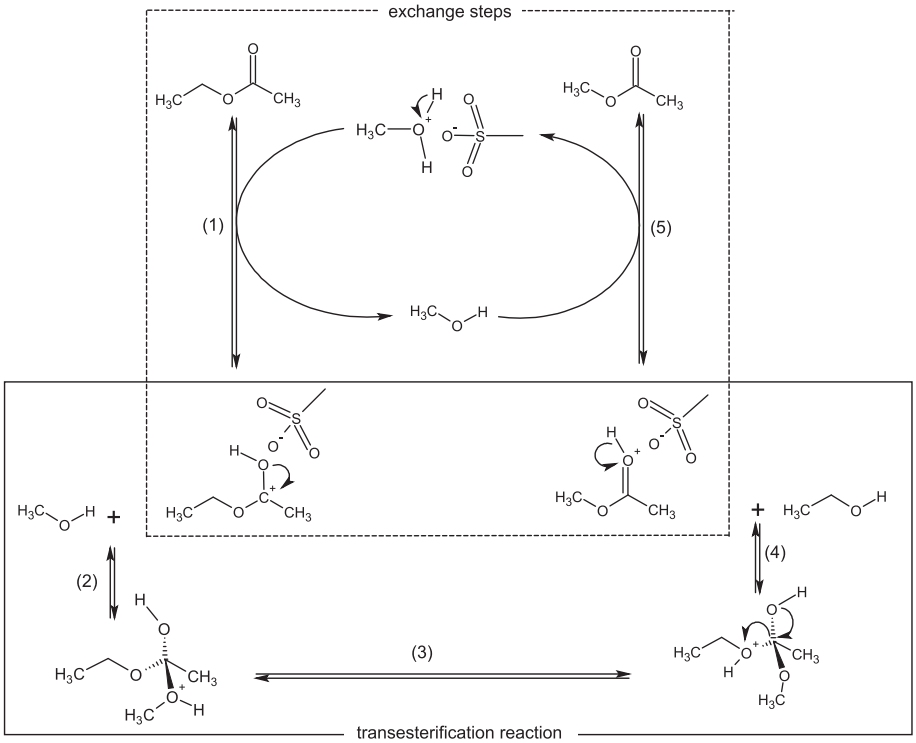

Fig. 5. Heterogeneous acid ion-exchange resin catalyzed reaction mechanism for ethyl acetate transesterification with methanol.

Table 4
Statistical evaluation of the adsorption and exchange based kinetic model for ethyl acetate transesterification with methanol on Lewatit K1221 at the operating conditions reported in Table 2.

Model	Number of statistically significantly estimated (total) parameters	RSSQ	*F*
Adsorption based model (Eq. (3))	4 (4)	27.2	62,000
Exchange based model (Eq. (4))	4 (4)	23.7	71,000

also developed for the present assessment of the experimental data on the gel versus the macroporous resins. The performance of the novel reaction rate equation will be compared with that of Eq. (3), see Section 4.1.3.

4.1.2. Exchange based model

The Flory–Huggins theory of polymer swelling is the most advanced methodology for rationalizing the partitioning of components between the bulk liquid of a multicomponent mixture and the resins' internal volume [19]. In the framework of this theory, the uptake of solvent species is considered as a phase equilibrium requiring suitable expressions for the thermodynamic activities as a function of the phase composition in the resin. Given the typically high molar methanol excess in the experiments performed in this work, the benefits of using the Flory–Huggins theory are expected to be limited and, hence, so called 'exchange coefficients' are employed to account for the resins' swelling and describe the reaction kinetics of the transesterification catalyzed by different resin types.

When adsorption based models are applied to account for catalysis by macroporous and gel type resins, the adsorption equilibrium coefficient accounts both for adsorption on the active sites and gel particle swelling. The first step in an adsorption based model is the adsorption of a component on the empty active site of the resin [5], whereas in the exchange based model it is assumed that all active sites are always occupied and, hence, the first step is an exchange from 2 components on the active sites of the resin, see Fig. 5. The exchange based kinetic model for the transesterification catalyzed by gel and macroporous resins is built on the schematic representation of the swelling of the two types of resins, given in Fig. 2. The adsorption based kinetic model, as originally proposed in our previous work [5] (Eq. (3)), is hence, extended with the following hypotheses:

(i) The swelling of the resin is attributed to the strong sorption of the solvent, i.e., methanol. All active sites of the resin are occupied, (initially) by protonated methanol (Fig. 5).

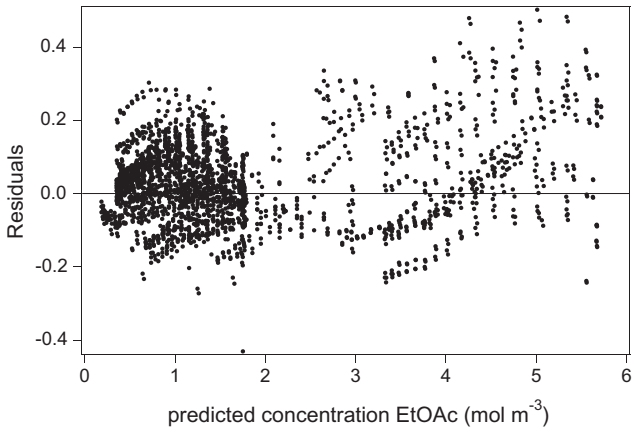

Fig. 6. Residual figure for the ethyl acetate concentration in its transesterification with methanol catalyzed by Lewatit K1221 at the operating conditions reported in Table 2. The simulated values are obtained using Eq. (4) with the parameter estimates reported in Table 5.

(ii) The esters, i.e. ethyl and methyl acetate, undergo a proton exchange with the protonated methanol on the active sites, equilibrium is assumed for this exchange see Fig. 5; steps (1) and (5) for the transesterification reaction to proceed.

These hypotheses lead to the reaction mechanism shown in Fig. 5 and the corresponding rate equation with the surface reaction as the rate-determining step (step (3)):

$$r = \frac{k_{SR} K_{EtOAc} \left(a_{EtOAc} - \frac{1}{K_{eq}} \frac{a_{EtOH} a_{MeOAc}}{a_{MeOH}} \right)}{1 + \frac{K_{EtOAc} a_{EtOAc}}{a_{MeOH}} + \frac{K_{MeOAc} a_{MeOAc}}{a_{MeOH}}} \quad (4)$$

with k_{SR} the surface reaction rate coefficient, K_i the exchange equilibrium coefficient of component i, K_{eq} the equilibrium coefficient of the overall reaction and a_i the bulk activity of component i. The derivation of Eq. (4) is included in Appendix A.

The model parameters in the above kinetic equation are the surface reaction rate coefficient, k_{SR}, the activation energy, E_A, and the exchange equilibrium coefficients of ethyl and methyl acetate, K_{EtOAc} and K_{MeOAc}.

The exchange between ethanol and methanol on an active site is not considered in the model. Ethanol is less polar due to the longer alkyl chain compared to methanol and, hence, the driving force for this exchange is limited. A potential exchange with ethanol would not contribute significantly to the calculated reaction rate and, hence, ethanol is assumed to be instantaneously released in the bulk.

4.1.3. Model discrimination between exchange and adsorption based model for the transesterification reaction catalyzed by Lewatit K1221

The adsorption (Eq. (3)) and the exchange based model (Eq. (4)), are mathematically quite similar. Both models consider the same driving force and have an adsorption term that comprises three terms. Where the latter correspond to the adsorption of the alcohols in the adsorption model, in the exchange based model they correspond to protonated methanol, methyl and ethyl acetate. The exchange coefficients in the denominator of rate equation Eq. (4) correspond to the ratio of the adsorption coefficient of the concerned component to the adsorption coefficient of methanol. Comparing the two denominators, the factor 1 in Eq. (3) is replaced by a_{MeOH} in Eq. (4) and the activity and the adsorption of the alcohols in Eq. (3) are replaced by the activity and the exchange of the esters in Eq. (4). The statistical evaluation of the adsorption and the exchange based model is shown in Table 4.

All parameters were estimated significantly different from zero. The obtained *F* values for the global significance of the regression range from 62,000 to 71,000, and exceed the tabulated *F* value by far. The best performing model in simulating experimentally observed kinetics is the exchange based model which has the lowest residual sum of squares (23.7) and the highest *F*-value (71,000). Although it does not outperform the adsorption based model on the reference resin, the good statistics combined with the physicochemical meaning of the model, as explained above, make the exchange based model the preferred one for further assessment of the transesterification kinetics on the various resins considered. A corresponding residual figure for the exchange based model is presented in Fig. 6, and indicates the overall adequacy of the model.

A similar model discrimination for the macroporous resins, which also results in the selection of the exchange based mechanism as the most adequate one, is included in the Supporting Information.

4.2. Quantitative assessment of the differences observed between Lewatit K1221, Lewatit K2640, Lewatit K2629 and Amberlyst 15

Regression of the experimental runs reported in Section 3.2 by minimizing the objective function (Eq. (2)) resulted in estimates

Table 5
Kinetic parameter and ion-exchange equilibrium coefficient estimates and statistical evaluation for the exchange-based Eley-Rideal model (Eq(4)) for ethyl acetate transesterification with methanol on the resins reported in Table 1 at the operating conditions reported in Table 2.

Resin	Kinetic parameters		Exchange equilibrium coefficients		Statistical evaluation		
	$k_{SR_{Tref}}$ (10^{-3} mol kg_{cat}^{-1} s^{-1})	E_A (kJ mol^{-1})	K_{EtOAc}	K_{MeOAc}	N	RSSQ	F
K1221	52.7 ± 0.3	48.7 ± 0.9	1.15 ± 0.14	4.87 ± 0.38	1282	24	71,000
K2629	9.2 ± 1.0	49.7 ± 2.0	2.54 ± 0.35	9.04 ± 2.03	702	2	125,000
K2640	14.5 ± 4.1	42.9 ± 5.6	1.86 ± 0.67	6.26 ± 1.90	233	2	18,000
Amberlyst 15	10.3 ± 7.5	52.3 ± 6.6	1.36 ± 0.99	0.90 ± 6.04	129	6	35,000

for the 4 parameters of Eq. (4) ($k_{SR_{Tref}}$, E_A, K_{EtOAc} and K_{MeOAc}). The obtained parameter estimates and the statistical performance of the exchange model for the gel and macroporous resins are shown in Table 5. Within the limited temperature range of 303–333 K, the temperature dependence of the exchange equilibrium coefficients is not considered.

The model adequately describes the experimental data on all resins very well. The global significance of the regression which is assessed by the F value, ranges from 18,000 to 125,000. This value clearly exceeds the tabulated F value and, hence, the regression is globally significant for all four resins. Figs. 1–4 illustrate the good agreement between the model simulations and the experimental data.

Considering the individual confidence intervals, all activation energies are approximately equal to 49 kJ mol^{-1}, irrespective of the resin used. These activation energies are, de facto, a composite activation energy, E_A^{comp}, comprising the two elementary steps involved in the reaction mechanism, i.e., the proton exchange between ethyl acetate and protonated methanol, $\Delta H_{exchange}$, and the actual surface reaction, E_A [54]:

$$E_A^{comp} = E_A + \Delta H_{exchange} \quad (5)$$

The true activation energy and the standard exchange enthalpy can, hence, not be estimated as separate parameters. The similar values obtained for the composite activation energies indicate that the energy barriers to be surmounted by the reacting components are comparable for all the catalysts. This can be explained by the formation of similar interactions on the same functional groups for all 4 catalysts. The composite activation energy obtained on Lewatit K2640 being on the lower side of this range may be attributed to the polysulfonated character of this resin and a corresponding, small effect on the exchange enthalpy. For a transesterification catalyzed with an acid ion-exchange resin similar (composite) activation energy values were published in literature [9,14,32,53,55].

The gel type catalyst, Lewatit K1221, has a $k_{SR_{T_{ref}}}$ at 328.38 K that is 3–4-fold higher than that of the macroporous catalysts, Lewatit K2640, K2629 or Amberlyst 15, as could be expected from the experimental data and the similar composite activation energies. The pre-exponential factor of the rate coefficient accounts for the entropy difference between the reactants and the transition state species, as well as for the number of active/accessible sites. Since macroporous resins swell less than gel type ones, the number of accessible active sites will typically be lower for the former compared to the latter, see Fig. 2. It, hence, makes sense that the pre-exponential factor obtained for the macroporous resins is lower than that for the gel type resin. For Amberlyst 15 and Lewatit K2629, both with a total number of active sites of 4.8 meq/kg_{resin}, the same pre-exponential factor is obtained. Nevertheless, the confidence interval of $k_{SR_{Tref}}$ for Amberlyst 15 is quite wide. Because of the higher divinylbenzene content of the latter, i.e., 20% compared to 18% for Lewatit K2629, less swelling has been observed on Amberlyst 15, see Section 3.1, and, hence, the true value for the pre-exponential factor on Lewatit K2629 is expected to be higher than the true one on Amberlyst 15. For Lewatit K2629 and Lewatit K2640, both with a crosslinking degree of 18%, the true value of the pre-exponential factor on Lewatit K2629 will rather be lower than on Lewatit K2640, because of the higher total number of active sites of the latter, i.e. 5.2 meq/kg_{resin}, due to the polysulfonation .

The exchange equilibrium coefficients, K_{MeOAc} and K_{EtOAc} have the same order of magnitude for all catalysts. The value of K_{MeOAc} for Amberlyst 15 is not significantly different from zero (t-value of 0.52), which is attributed to the limited number of experimental data, the correspondingly limited range of operating conditions as well as to the relatively low conversions obtained on Amberlyst 15 and, hence, the less significant presence of methyl acetate in the reaction mixture. The exchange equilibrium coefficients are slightly higher for the macroporous resins compared to the gel type resin, suggesting that the sorption of methanol on the gel type resin is more pronounced than on the macroporous resins as confirmed by the volumetric swelling experiments, see Section 3.1. The ratio between the methyl and ethyl acetate exchange coefficient is identical for all resins and amounts to 4 approximately. This reflects the chemical similarity of the resins. The additional methylene group in ethyl acetate results in a lower exchange equilibrium coefficient, which is in agreement with the results obtained by Ali et al. [9] for butyl acetate versus ethyl acetate.

4.3. Assessment of molar fractions within the resin

In order to obtain more insight in how the model quantifies the phenomena occurring at the active sites of the resin, the ethyl and methyl acetate fractions in the resin, i.e., θ_{EtOAc^*} and θ_{MeOAc^*}, as well as the methanol fraction in the resin, θ_{MeOH^*}, can be calculated employing the exchange based kinetic model, making use of the site balance and the quasi-equilibrium assumption, see Eq. (6)–(9).

$$1 = \theta_{MeOH^*} + \theta_{EtOAc^*} + \theta_{MeOAc^*} \quad (6)$$

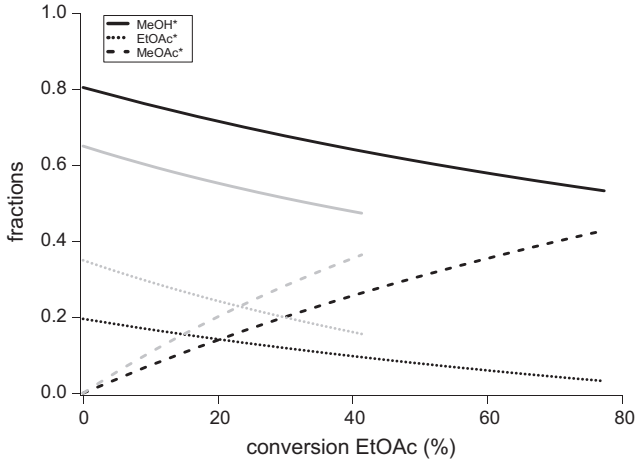

Fig. 7. Simulated (ER_exchange model, Eq (4), with parameters as reported in Table 5) molar fractions in the resin as a function of the ethyl acetate conversion at all temperatures and MeOH:EtOAc ratio = 10:1, catalyzed by Lewatit K1221 (black) and by Lewatit K2629 (grey). (EtOAc* and MeOAc* chemisorbed fractions of ethyl acetate and methyl acetate, respectively; MeOH* fraction of sites covered by methanol).

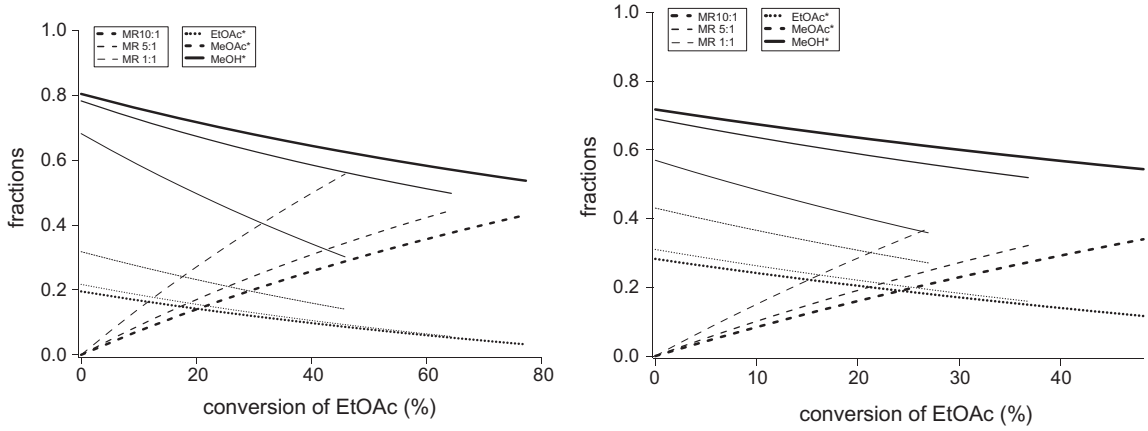

Fig. 8. Simulated (ER_exchange model, Eq (4), with parameters as reported in Table 5) fractions as a function of the ethyl acetate conversion at 333 K with various MeOH:EtOAc ratios (legend), catalyzed by Lewatit K1221 (left) and by Lewatit K2640 (right). (EtOAc* and MeOAc* chemisorbed fractions of ethyl acetate and methyl acetate, respectively; (MeOH*) fraction of sites covered by methanol).

$$\theta_{MeOH^*} = \frac{1}{1 + \frac{K_{EtOAc} a_{EtOAc}}{a_{MeOH}} + \frac{K_{MeOAc} a_{MeOAc}}{a_{MeOH}}} \quad (7)$$

$$\theta_{EtOAc^*} = \frac{\frac{K_{EtOAc} a_{EtOAc}}{a_{MeOH}}}{1 + \frac{K_{EtOAc} a_{EtOAc}}{a_{MeOH}} + \frac{K_{MeOAc} a_{MeOAc}}{a_{MeOH}}} \quad (8)$$

$$\theta_{MeOAc^*} = \frac{\frac{K_{MeOAc} a_{MeOAc}}{a_{MeOH}}}{1 + \frac{K_{EtOAc} a_{EtOAc}}{a_{MeOH}} + \frac{K_{MeOAc} a_{MeOAc}}{a_{MeOH}}} \quad (9)$$

The molar fractions in the resin as a function of conversion at different temperatures and different initial molar methanol to ethyl acetate ratios are shown in Figs. 7 and 8 for gel and macroporous resins, respectively.

At the start of an experiment catalyzed by K1221 with an initial methanol to ethyl acetate molar ratio of 10:1, 80% and 20% of the sites is covered with methanol and ethyl acetate, independently of the temperature, see Fig. 7. At 44% ethyl acetate conversion, the methanol, ethyl acetate and methyl acetate fractions amount to 64%, 10% and 26%. Given the absence of a temperature effect on the exchange coefficients, also at higher conversions the molar fractions within the resin are independent of the temperature. Of course, at higher temperatures, the same conversion is reached at a shorted batch time, see Fig. 3. A similar evolution of the molar fractions within the resin as a function of the conversion is obtained for the macroporous resins, see Fig. 7 for Lewatit K2629 as an example. Due to the higher exchange equilibrium coefficients for the esters on K2629, the initial methanol fraction is lower than that on the gel type resin. The same effect is still visible at 44% ethyl acetate conversion, with methanol, ethyl acetate and methyl acetate fractions amounting to 48%, 16% and 36%.

The effect of the initial molar methanol to ethyl acetate ratio is investigated at 333 K. The fractions obtained at an initial molar ratio of 10:1 and at an ethyl acetate conversion of 77%, are 54%, 3% and 43% for methanol, ethyl acetate and methyl acetate. At a molar ratio of 5:1, the results are comparable. An increase of initial molar ratio from 5:1 to 10:1, does not lead to appreciably different fractions. At an initial molar ratio of 1:1, the methanol fraction in the resin is lower, due to its lower liquid bulk concentration, i.e., 68% at the start and 30% at 46% ethyl acetate conversion. The ethyl and methyl acetate fractions are correspondingly higher, i.e., 32% and 0% at the start and 14% and 56% at 46% ethyl acetate conversion. Nevertheless, methanol remains the most abundant species within the resin, except at higher batch times with the lowest initial molar ratios. The different fractions obtained with initial molar ratio 1:1 and 5:1 or 10:1 are also due to differences in the activity coefficients of methanol, methyl and ethyl acetate. Similar trends are observed for the macroporous resins, see Fig. 8 (right), which are in line with the experimental observations discussed in Section 3.2.

6. Conclusions

Acid ion-exchange resins can be used as catalysts for ethyl acetate transesterification with methanol to methyl acetate and ethanol. Due to the chemical similarity between the considered resins, differences in observed reaction rates were mainly related to the accessibility of the active sites. The latter is inversely proportional with the extent of cross-linking by divinylbenzene due to the corresponding swelling behavior of the resins. Gel type resins are subject to more pronounced swelling compared to macroporous ones due to the rigidity induced by the higher divinylbenzene cross linking in the latter. Resin swelling is also more pronounced when it is in contact with more polar solvents. The number of accessible active sites as well as their strength can, to a less pronounced extent, also be enhanced by polysulfonation.

A novel kinetic model, implicitly accounting for resin swelling was developed with the following assumptions:

(1) all active sites are occupied by either methanol, ethyl or methyl acetate,
(2) the exchange between protonated methanol and the esters is quasi equilibrated, and
(3) an Eley–Rideal type surface reaction between protonated ethyl acetate methanol from the bulk occurs as the rate-determining step,

and allowed interpreting the observed differences between the various gel and macroporous resins investigated in this work. The latter were mainly reflected in the estimated rate coefficients. Just like the transesterification rates, the reaction rate coefficients were found to be proportional to the accessibility of the active sites and, hence, inversely proportional to the cross-linking degree. The activation energy amounts to 49 kJ/mol independent of the considered resin and is an indication of their chemical similarity. Methanol is the most abundant surface intermediate, followed by methyl and ethyl acetate respectively. Due to the additional methylene group, the ethyl acetate exchange equilibrium coefficient is a factor 3–4 smaller than that of methyl acetate. The presented modelling methodology has resulted in an accurate simulation of the kinetic

behavior of different types of resins and allowed developing a physically sound interpretation of the reaction kinetics and mechanism.

Acknowledgments

The Research Fund of the University College Ghent and the faculty of Engineering and Architecture of Ghent University are acknowledged for their financial support. Lanxess is acknowledged for providing the ion-exchange resins.

Appendix A. Supplementary material

Supplementary material associated with this article can be found, in the online version, at http://dx.doi.org/10.1016/j.cej.2013.12.025.

References

[1] S.H. Ali, Kinetics of catalytic esterification of propionic acid with different alcohols over Amberlyst 15, Int. J. Chem. Kinet. 41 (2009) 432–448.
[2] T.F. Dossin, M.F. Reyniers, R.J. Berger, G.B. Marin, Simulation of heterogeneously MgO-catalyzed transesterification for fine-chemical and biodiesel industrial production, Appl. Catal., B 67 (2006) 136–148.
[3] J.A. Melero, L.F. Bautista, G. Morales, J. Iglesias, R. Sanchez-Vazquez, Biodiesel production from crude palm oil using sulfonic acid-modified mesostructured catalysts, Chem. Eng. J. 161 (2010) 323–331.
[4] A. Chakrabarti, M.M. Sharma, Cationic ion-exchange resins as catalyst, React. Polym. 20 (1993) 1–45.
[5] E. Van de Steene, J. De Clercq, J.W. Thybaut, Adsorption and reaction in the transesterification of ethyl acetate with methanol on Lewatit K1221, J. Mol. Catal. A: Chem. 359 (2012) 57–68.
[6] B. Saha, M. Streat, Transesterification of cyclohexyl acrylate with n-butanol and 2-ethylhexanol: acid-treated clay, ion exchange resins and tetrabutyl titanate as catalysts, React. Funct. Polym. 40 (1999) 13–27.
[7] D.M. Alonso, M.L. Granados, R. Mariscal, A. Douhal, Polarity of the acid chain of esters and transesterification activity of acid catalysts, J. Catal. 262 (2009) 18–26.
[8] V.K.S. Pappu, A.J. Yanez, L. Peereboom, E. Muller, C.T. Lira, D.J. Miller, A kinetic model of the Amberlyst-15 catalyzed transesterification of methyl stearate with n-butanol, Bioresour. Technol. 102 (2011) 4270–4272.
[9] S.H. Ali, O. Al-Rashed, F.A. Azeez, S.Q. Merchant, Potential biofuel additive from renewable sources – kinetic study of formation of butyl acetate by heterogeneously catalyzed transesterification of ethyl acetate with butanol, Bioresour. Technol. 102 (2011) 10094–10103.
[10] I. Zielinska-Nadolska, K. Warmuzinski, J. Richter, Zeolite and other heterogeneous catalysts for the transesterification reaction of dimethyl carbonate with ethanol, Catal. Today 114 (2006) 226–230.
[11] I. Zielinska-Nadolska, K. Warmuzinski, J. Richter, Screening of heterogeneous catalysts and kinetics of the transesterification reaction of dimethyl carbonate with ethanol, Inz. Chemiczna Process. 25 (2004) 1861–1866.
[12] B. Saha, M.M. Sharma, Reaction of dicyclopentadiene with formic acid and chloroacetic acid with and without cation-exchange resins as catalysts, React. Funct. Polym. 34 (1997) 161–173.
[13] L. Jimenez, A. Garvin, J. Costa-Lopez, The production of butyl acetate and methanol via reactive and extractive distillation. I. Chemical equilibrium, kinetics, and mass-transfer issues, Ind. Eng. Chem. Res. 41 (2002) 6663–6669.
[14] E. Bozek-Winkler, J. Gmehling, Transesterification of methyl acetate and *n*-butanol catalyzed by Amberlyst 15, Ind. Eng. Chem. Res. 45 (2006) 6648–6654.
[15] M. Di Serio, R. Tesser, L. Pengmei, E. Santacesaria, Heterogeneous catalysts for biodiesel production, Energy Fuels 22 (2008) 207–217.
[16] S. Steinigeweg, J. Gmehling, Transesterification processes by combination of reactive distillation and pervaporation, Chem. Eng. Process. 43 (2004) 447–456.
[17] R. Tesser, L. Casale, D. Verde, M. Di Serio, E. Santacesaria, Kinetics and modeling of fatty acids esterification on acid exchange resins, Chem. Eng. J. 157 (2010) 539–550.
[18] R. Tesser, M. Di Serio, L. Casale, L. Sannino, M. Ledda, E. Santacesaria, Acid exchange resins deactivation in the esterification of free fatty acids, Chem. Eng. J. 161 (2010) 212–222.
[19] N.G. Polyanskii, V.K. Sapozhnikov, New advances in catalysis by ion-exchange resins, Russ. Chem. Rev. 46 (1977) 445–476.
[20] G.M. Gusler, T.E. Browne, Y. Cohen, Sorption of organics from aqueous-solution onto polymeric resins, Ind. Eng. Chem. Res. 32 (1993) 2727–2735.
[21] T. Sainio, M. Laatikainen, E. Paatero, Phase equilibria in solvent mixture-ion exchange resin catalyst systems, Fluid Phase Equilib. 218 (2004) 269–283.
[22] S. Horstmann, T. Popken, J. Gmehling, Phase equilibria and excess properties for binary systems in reactive distillation processes Part I. Methyl acetate synthesis, Fluid Phase Equilib. 180 (2001) 221–234.
[23] R. Tesser, M. Di Serio, L. Casale, G. Carotenuto, E. Santacesaria, Absorption of water/methanol binary system on ion-exchange resins, Can. J. Chem. Eng. 88 (2010) 1044–1053.
[24] M. Mazzotti, B. Neri, D. Gelosa, A. Kruglov, M. Morbidelli, Kinetics of liquid-phase esterification catalyzed by acidic resins, Ind. Eng. Chem. Res. 36 (1997) 3–10.
[25] F. Helfferich, Ion Exchange, Dover Publications, 1995.
[26] A. Martinec, K. Setinek, L. Beranek, Effect of cross-linking on catalytic properties of macroporous styrene-divinylbenzene ion-exchangers, J. Catal. 51 (1978) 86–95.
[27] S.K. Ihm, J.H. Ahn, Y.D. Jo, Interaction of reaction and mass transfer in ion-exchange resin catalysts, Ind. Eng. Chem. Res. 35 (1996) 2946–2954.
[28] M.J. Lee, H.T. Wu, H.M. Lin, Kinetics of catalytic esterification of acetic acid and amyl alcohol over Dowex, Ind. Eng. Chem. Res. 39 (2000) 4094–4099.
[29] F. Lode, S. Freitas, M. Mazzotti, M. Morbidelli, Sorptive and catalytic properties of partially sulfonated resins, Ind. Eng. Chem. Res. 43 (2004) 2658–2668.
[30] S.K. Ihm, M.J. Chung, K.Y. Park, Activity difference between the internal and external sulfonic groups of macroreticular ion-exchange resin catalysts in isobutylen hydration, Ind. Eng. Chem. Res. 27 (1988) 41–45.
[31] J. Lilja, E. Murzina, H. Grenman, H. Vainio, T. Salmi, D.Y. Murzin, The selective sorption of solvents on sulphonic acid polymer catalyst in binary mixtures, React. Funct. Polym. 64 (2005) 111–118.
[32] D.E. Lopez, J.G. Goodwin, D.A. Bruce, Transesterification of triacetin with methanol on Nafion (R) acid resins, J. Catal. 245 (2007) 381–391.
[33] F.M.B. Coutinho, S.M. Rezende, B.G. Soares, Characterization of sulfonated poly(styrene-divinylbenzene) and poly(divinylbenzene) and its application as catalysts in esterification reaction, J. Appl. Polym. Sci. 102 (2006) 3616–3627.
[34] B.E. Poling, J.M. Prausnitz, J.P. O'Connell, The Properties of Gases and Liquids, McGraw-Hill, 2001.
[35] M. Schwaab, J.C. Pinto, Optimum reference temperature for reparameterization of the Arrhenius equation. Part 1: problems involving one kinetic constant, Chem. Eng. Sci. 62 (2007) 2750–2764.
[36] G.F. Froment, K.B. Bischoff, Chemical Reactor Analysis and Design, second ed., Wiley, 1990.
[37] W.E. Stewart, M. Caracotsios, Computer-Aided Modeling of Reactive Systems, Wiley-Interscience, 2008.
[38] A. Rehfinger, U. Hoffmann, Kinetics of methyl tertairy butyl ether liquid-phase synthesis cataalyzed by ion-exchange resin. 1. Intrinsic rate expression in liquid-phase activities, Chem. Eng. Sci. 45 (1990) 1605–1617.
[39] B. Corain, M. Zecca, P. Canton, P. Centomo, Synthesis and catalytic activity of metal nanoclusters inside functional resins: an endeavour lasting 15 years, Philos. Trans. R. Soc. A-Math. Phys. Eng. Sci. 368 (2010) 1495–1507.
[40] M. Mazzotti, A. Kruglov, B. Neri, D. Gelosa, M. Morbidelli, A continuous chromatographic reactor: SMBR, Chem. Eng. Sci. 51 (1996) 1827–1836.
[41] R. Zimehl, Flow microcalorimetry and competitive liquid sorption –II. Liquid sorption and wetting on macroreticular hydrophilic/hydrophobic networks, Thermochim. Acta 310 (1998) 207–215.
[42] Y.T. Tsai, H.M. Lin, M.J. Lee, Kinetics behavior of esterification of acetic acid with methanol over Amberlyst 36, Chem. Eng. J. 171 (2011) 1367–1372.
[43] B. Corain, P. Centomo, S. Lora, M. Kralik, Functional resins as innovative supports for catalytically active metal nanoclusters, J. Mol. Catal. A: Chem. 204 (2003) 755–762.
[44] P.F. Siril, A.D. Davison, J.K. Randhawa, D.R. Brown, Acid strengths and catalytic activities of sulfonic acid on polymeric and silica supports, J. Mol. Catal. A: Chem. 267 (2007) 72–78.
[45] P.F. Siril, D.R. Brown, Acid site accessibility in sulfonated polystyrene acid catalysts: calorimetric study of NH_3 adsorption from flowing gas stream, J. Mol. Catal. A: Chem. 252 (2006) 125–131.
[46] P.R. Siril, H.E. Cross, D.R. Brown, New polystyrene sulfonic acid resin catalysts with enhanced acidic and catalytic properties, J. Mol. Catal. A: Chem. 279 (2008) 63–68.
[47] E. Lotero, Y.J. Liu, D.E. Lopez, K. Suwannakarn, D.A. Bruce, J.G. Goodwin, Synthesis of biodiesel via acid catalysis, Ind. Eng. Chem. Res. 44 (2005) 5353–5363.
[48] M. Di Serio, R. Tesser, M. Dimiccoli, F. Cammarota, M. Nastasi, E. Santacesaria, Synthesis of biodiesel via homogeneous Lewis acid catalyst, J. Mol. Catal. A: Chem. 239 (2005) 111–115.
[49] E. Lotero, J.G. Goodwin, D.A. Bruce, K. Suwannakarn, Y.J. Liu, D.E. Lopez, The Catalysis of Biodiesel Synthesis, in: J.J. Spivey, K.M. Dooley (Eds.), Catalysis, vol. 19, Royal Soc Chemistry, Cambridge, 2006, pp. 41–83.
[50] U. Schuchardt, R. Sercheli, R.M. Vargas, Transesterification of vegetable oils: a review, J. Braz. Chem. Soc. 9 (1998) 199–210.
[51] M. Smith, J. March, March's Advanced Organic Chemistry: Reactions, Mechanisms, and Structure, Wiley-Interscience, 2007.
[52] H.T.R. Teo, B. Saha, Heterogeneous catalysed esterification of acetic acid with isoamyl alcohol: kinetic studies, J. Catal. 228 (2004) 174–182.
[53] B.Y. Xu, W.J. Zhang, X.M. Zhang, C.F. Zhou, Kinetic Study of transesterification of methyl acetate with *n*-butanol catalyzed by NKC-9, Int. J. Chem. Kinet. 41 (2009) 101–106.
[54] J.W. Thybaut, C.S.L. Narasimhan, G.B. Marin, J.F.M. Denayer, G.V. Baron, P.A. Jacobs, J.A. Martens, Alkylcarbenium ion concentrations in zeolite pores during octane hydrocracking on Pt/H–USY zeolite, Catal. Lett. 94 (2004) 81–88.
[55] S.H. Ali, S.Q. Merchant, Kinetics of the esterification of acetic acid with 2-propanol: impact of different acidic cation exchange resins on reaction mechanism, Int. J. Chem. Kinet. 38 (2006) 593–612.